

Raman Microscope

ATR8800C

Features

- Fully automatic Raman imaging experiment, automatic focusing and automatic scanning.
- Confocal optical path design (confocal optional).
- Supports up to 4 excitation wavelengths for Raman.
- Ultra-long focal length and high-resolution design.
- Rotating grating design, integrating large range and high resolution.
- Sealed hatch design, the experiment is not affected by ambient light.
- Ultra-high sensitivity, signal-to-noise ratio >6000:1
- Ultra-large range imaging (100X100mm), automatic image stitching.
- Unique software controls switching light path.
- Quick positioning, quickly find the focus position.
- High-quality objective lens, micron-level light spot.
- 5 million camera, clear and accurate images.
- USB3.0 interface directly connected to computer.

Application

- Nanoparticles and new materials
- Research institute research
- Biology
- Forensic Medicine Identification
- Material science
- Medical Immunoassay
- Agriculture and food identification
- Gem and inorganic mineral identification
- Environment

Description

ATR8800 C series micro-Raman spectrometer integrates up to 4 lasers and combines the advantages of both microscopes and Raman spectrometers. The micro-Raman detection platform makes it possible to "what you see is what you measure", and the visualization is accurate. The positioning Raman detection platform allows observers to detect Raman signals of different surface states on the sample, and can simultaneously display the micro-area morphology at the detected location on the computer, which greatly facilitates Raman micro-area detection.

The entire ATR8800 series can perform fully automatic focusing, fully automatic scanning, and one-click operation. It can perform batch experiments, uniformity scanning, etc. without waiting, and can obtain highly reliable scanning imaging Raman data;

ATR8800 is equipped with spectrometers with different focal lengths to meet different resolution requirements. ATR8800 is also equipped with an objective lens specially designed for the Raman system, which makes the laser spot close to the diffraction limit. The focus information is accurately and intuitively displayed on the computer through a 5 million camera. It overcomes the problem in ordinary Raman systems that the focal plane for collecting Raman signals is slightly higher or slightly lower than the actual optimal focal plane, thereby improving the quality of the Raman spectrum.

ATR8800 perfectly solves the loss of optical path during camera imaging and realizes the separation of camera imaging and Raman signal collection, thereby obtaining the best signal strength. At the same time, ATR8800 uses high-performance Raman specially optimized for micro-Raman systems. It is industry-leading in terms of sensitivity, signal-to-noise ratio, stability, etc., providing a strong guarantee for Raman research.



Product data information i
publication data. Products conform to
specifications per the terms of Optosky Standard
warranty.

1. Working principle

Raman spectroscopy can quickly and non-destructively detect many intrinsic information of materials, such as the crystal structure of the material, electron-phonon coupling, electronic band structure, phonon energy dispersion and other information. Because of its high resolution, it is one of the most important means in the research of carbon materials. Since the discovery of graphene, Raman spectroscopy has been widely used in the study of graphene, such as: using Raman spectroscopy to identify graphene. The number of layers, doping types, structural defects, interlayer stacking of carbon atoms, in-plane vibration of SP² carbon atoms, etc., therefore using Raman spectroscopy to study graphene has unique advantages.

1.1 Raman spectroscopy analysis of graphene layers

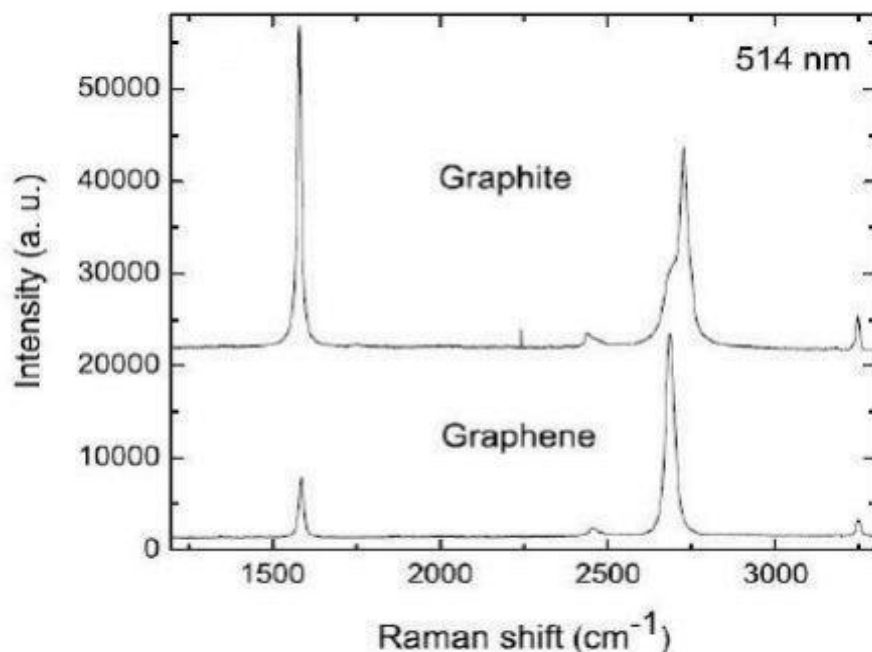


Figure 1 Comparison of Raman spectra of graphene and graphite

For the Raman spectrum of high-quality single-layer graphene, the most significant features are the G peak (1580 cm^{-1}) and the 2D peak (2700 cm^{-1}). Among them, the G peak can well reflect the symmetry and crystallization degree of graphene; the 2D peak can reflect the energy band structure of graphene. By comparing the Raman spectra of single-layer graphene and thicker graphite in Figure 1, it is found that the two have G peaks with similar shapes. Although the intensities are different, they are both single peaks; however, the 2D peak of single-layer graphene is a symmetrical single peak, while the 2D peak of graphite is not a single peak, and the 2D peaks of the two substances are quite different. In addition, no D peak was observed in single-layer graphene, indicating that the integrity of the test sample was good and there were no lattice defects.

Ferrari et al. studied the Raman spectra of graphene with different layers. The results are shown in Figure 2. They found that **as the number of graphene layers increases, the 2D peak moves to the direction of high wave numbers (red shift phenomenon), and the half-maximum width gradually becomes wider. The G peak intensity increases linearly with the increase in layer number.** Therefore, the number of graphene layers can be identified through this feature. However, experiments have shown that this conclusion is only true within 10 layers. When it exceeds 10 layers, as the number of layers increases, due to the multi-level reflection of the Raman signal in graphene and the multi-level interference of the incident light, the G peak intensity gradually decreases and weakens.

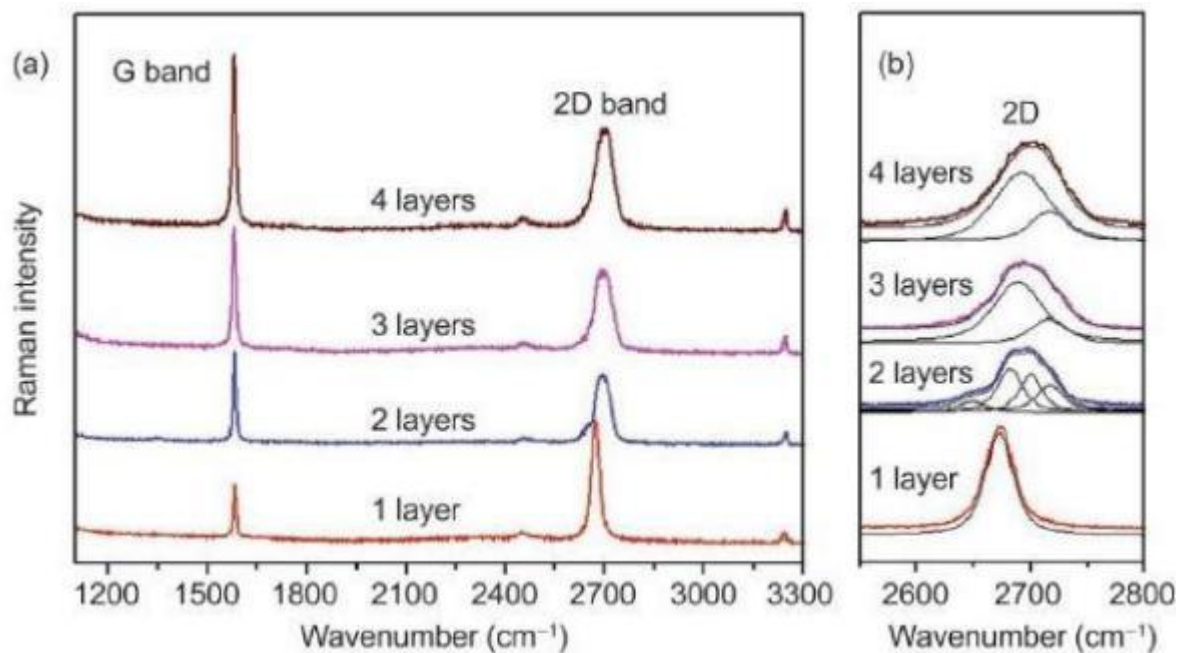


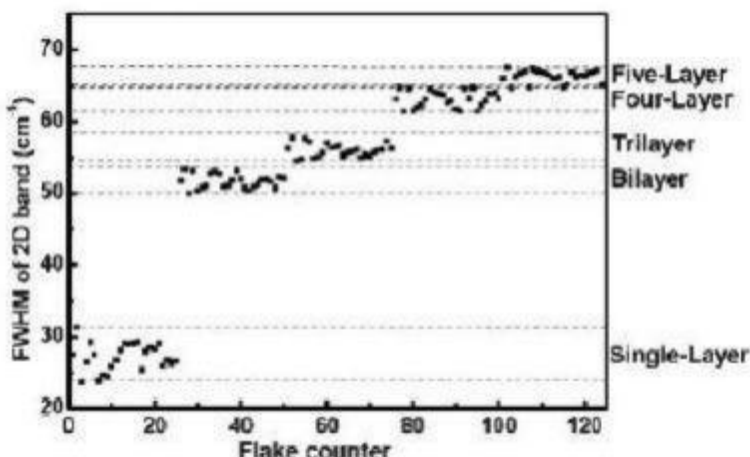
Figure 2 (a) Raman spectra of graphene with different layers [28]; (b) 2D peak fitting process of graphene with different layers

Y. Hao et al. further studied the Raman spectra of graphene with different layers and concluded that the number of graphene layers can be **identified by the half-width of the 2D peak**. The half-width of the 2D peak of the Raman spectrum of graphene with different layers was tested. As shown in Figure 3, the single-layer graphene is 20cm⁻¹ - 30cm⁻¹, the double-layer graphene is 50cm⁻¹ - 54cm⁻¹, and the three-layer graphene is 55cm⁻¹ - 58cm⁻¹. Four-layer graphene is between 62cm⁻¹ and 65cm⁻¹, and five-layer graphene is between 65cm⁻¹ and 67cm⁻¹. It was found that the range of the half-height width of graphene with different layer numbers does not overlap, **so the number of graphene layers can be determined by the half-height width of the 2D peak**. Although the positions and intensities of the 2D peaks of different graphene are different, the range of the half-width of graphene with the same number of layers is certain. Factors such as charge doping and laser incident energy will not affect the half-width.

Note: This method can only identify the thickness of graphene within 5 layers. Because the number of layers is greater than 5, the signal of graphene is similar to that of graphite, making it difficult to distinguish.

Therefore, **the peak shape and half-maximum width of the 2D peak are good ways to identify the number of graphene layers**.

Figure 3 The relationship between the half-width of the 2D peak of the Raman spectrum of graphene



and the number of layers of graphene with different layers

1.2 Defect analysis of graphene

Due to the special energy band structure of graphene, the switching ratio of field effect devices using it as a channel is extremely low. Therefore, a series of methods have been used to open the band gap to increase its light-on ratio, but these methods will introduce defects. Previous studies have shown that graphene containing defects will have a Raman D peak at around 1350 cm⁻¹, so the intensity of the D peak and the intensity ratio of the D peak to the G peak are often used to detect defects in graphene, and we can further derive the density of defects.

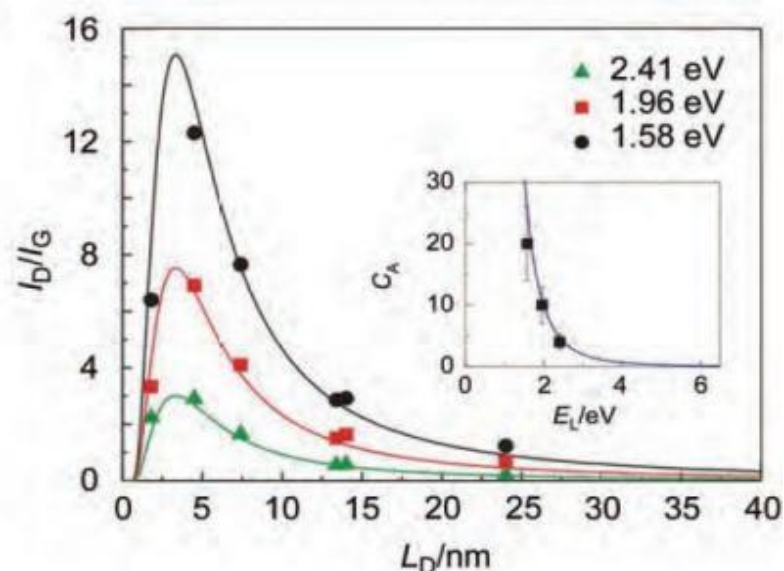


Figure 4 The relationship between ID /IG and LD

The intensity ratio ID / IG of graphene Raman D peak and G peak is an important parameter to measure the defect density. Assuming that the defects in graphene are very small, they can be regarded as zero-dimensional point defects. The distance between two zero-dimensional point defects is recorded as LD. By calculating the intensity ratio ID / IG, LD can be obtained, and further find the defect density of graphene. As shown in Figure 4, the intensity ratio of D peak to G peak is ID/IG.

It increases with the decrease of the distance LD between defect points. When LD is about 3 nm, ID/IG reaches the maximum, and when the distance between defects continues to decrease, the effect of defects on the D peak will no longer be independent. , the sp² carbon area gradually decreases until the six-membered ring opens, which will cause the G peak intensity to decrease quickly.

In addition, in the Raman spectrum of graphene containing defects, D peak and D' peak will appear, and the intensity ratio ID / IG' between the two defect peaks is related to the type of graphene surface defects. Studies have shown that if defects are caused by holes, the ratio is about 7; if defects are caused by sp³ hybridization, ID / IG' can reach a maximum of 13; and if defects are caused by graphene edges, the ratio is about 3.5.

1.3 Doping analysis of graphene

In addition to the crystal structure of graphene itself, the doping effect of the substrate charge will also affect its Raman spectrum. For example, doping graphene through gate voltage modulation can adjust the position of the Fermi level of graphene and change the graphene. The Raman spectrum is shown in Figure 5. And it is concluded that n-type and p-type doping will cause the G peak of single-layer graphene to be blue-shifted, while the 2D peak will be red-shifted when n-type doped, and blue-shifted when p-type doped.

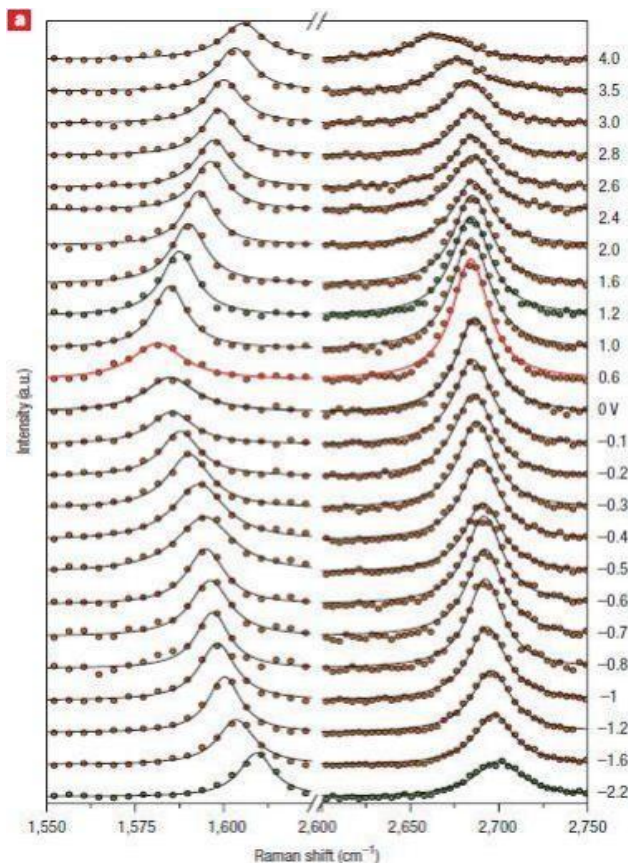


Figure 5 The relationship between graphene Raman spectrum and gate voltage after applying gate voltage

1.4 Effect of stress on graphene Raman spectrum

Stress has a great influence on the Raman characteristic peaks of graphene. Even very weak stress will cause obvious peak shifts in its Raman spectrum. Figure 6 shows the relationship between the Raman G peak position and the

2D peak position of graphene with different layer numbers as a function of stress. It can be seen that when stress is applied to graphene, its Raman G peak and 2D peak both shift to low wave numbers with the increase of stress. When the stress is released, the peak position of the Raman characteristic peak will blue-shift to when it is not stressed. The position (shown as the green dot in Figure 6 (b)).

Through further research, del Corro found that the direction of displacement is related to the type of stress. **When graphene is subjected to compressive stress, its characteristic Raman peak shifts blue due to the reduction in the spacing between carbon atoms.** When it is subjected to tensile stress, **the Raman peak Characteristic peaks are red-shifted. Research shows that applying tensile stress to graphene can controllably adjust its band gap.**

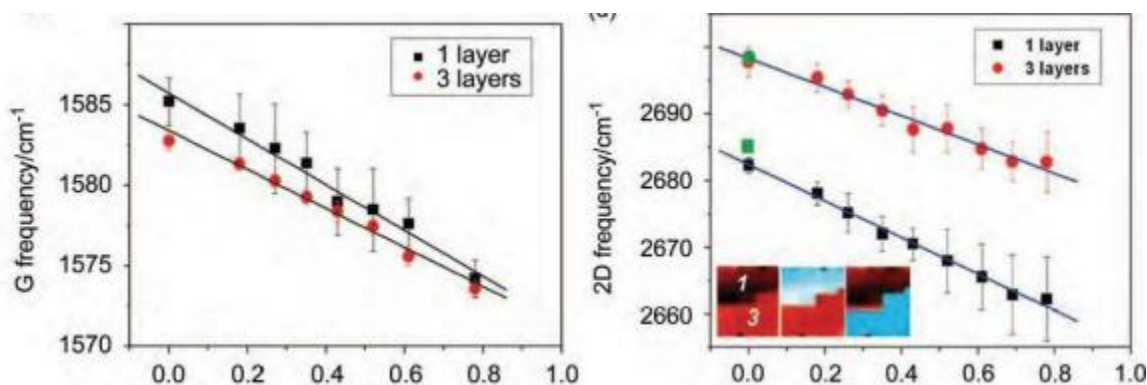


Figure 6 The relationship between the Raman peak position of graphene and the stress. (a) G peak; (b) 2D peak shift

1.5 Effect of substrate on Raman spectrum of single-layer graphene

Single-layer graphene on a SiO₂/Si substrate with a specific thickness can be observed through optical microscopy, so when we use Raman spectroscopy to study graphene, we mostly use the standard SiO₂ (300nm)/Si substrate. However, depending on the research content, different substrates need to be selected. Figure 7 represents the Raman spectra of single-layer graphene on different substrates. Figure 8 summarizes the peak positions and half-height widths of the 2D peak and G peak on different substrates. It can be seen that the peak position and half-height width of the G peak of graphene on different substrates are very close, which shows that graphene prepared by mechanical exfoliation is similar to The interaction between the substrates is weak, and the Raman characteristic peaks on different substrates will not fluctuate much. The peak positions of the 2D peak and G peak of the single-layer graphene epitaxially grown on the SiC substrate are obviously different from those prepared by the mechanical exfoliation method. This is due to the stress effect of the substrate. Figure 8 shows the Raman information of single-layer graphene prepared by different methods, including the half-height width and peak position of G and 2D peaks. Due to differences in the interaction between graphene and the substrate, doping concentration, etc. of different substrates, Therefore, there are great differences between the graphene Raman G peak and 2D peak on different substrates.

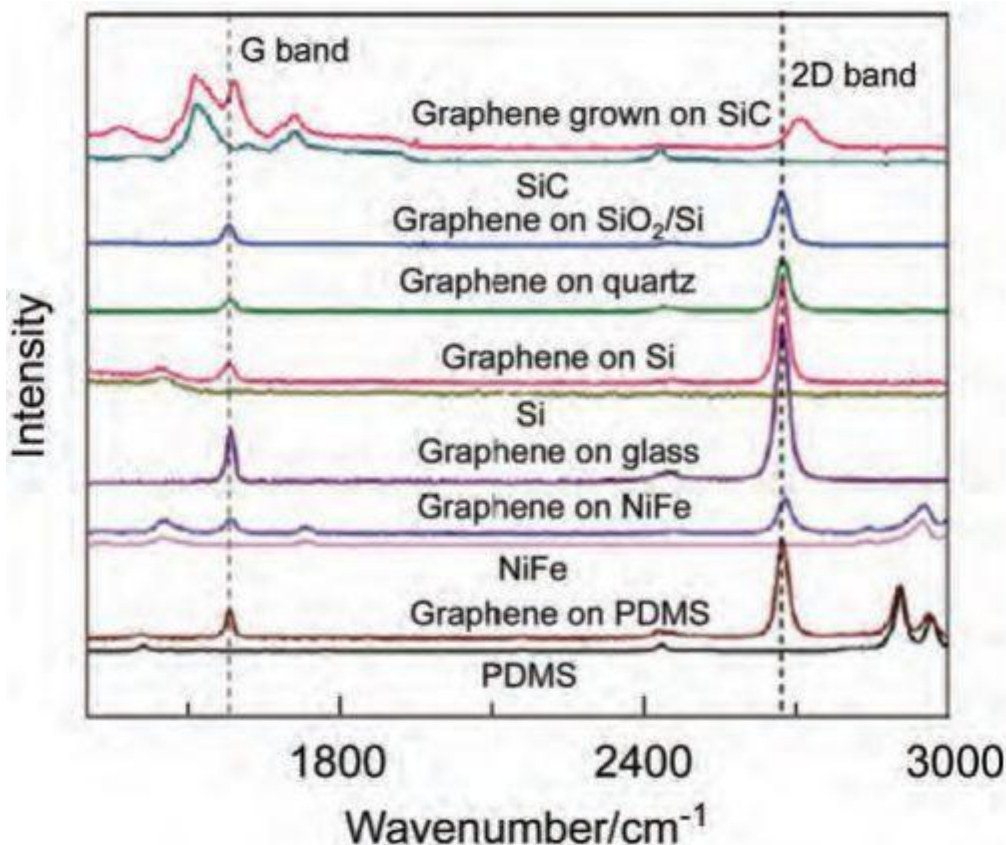


Figure 7 Raman spectra of single-layer graphene on different substrates

Substrate	G band		G' band	
	Position/cm ⁻¹	FWHM/cm ⁻¹	Position/cm ⁻¹	FWHM/cm ⁻¹
SiC	1591.5	31.3	2710.5	59.0
SiO ₂ /Si	1580.8	14.2	2676.2	31.8
Quartz	1581.9	15.6	2674.6	29.0
Si	1580	16	2672	28.3
PDMS	1581.6	15.6	2673.6	27
Glass	1582.5	16.8	2672.8	30.8
NiFe	1582.5	14.9	2678.6	31.4
GaAs	1580	15	—	—
Sapphire (0001)	1590.3	8.0	2678.4	28
Sapphire (11-20)	1586.4	10	2677.6	27
Sapphire (1-102)	1585.8	11	2677.1	29
ITO plate	1576	—	2665	—

Figure 8 Peak positions and half-peak widths of the Raman G peak and 2D peak of single-layer graphene on different substrates

2. Technical parameters

Table 1 ATR8800 performance parameters

ATR8800 Performance parameters	
Excitation wavelength	266、325、532、638、785、1064nm Optional, integrate up to 4 excitation wavelengths simultaneously
Laser power	266nm: 30 mW 325nm: 30mW 532nm: 100mW 633nm: 80mW 638nm: 80mW 785nm: 350mW 1064nm: 500mW
Spectrometer spectroscopy	Asymmetric C-T optical path
Spectrometer focal length	350mm、510mm、810mm Optional
Number of built-in gratings	Standard configuration: 3 pieces; 300 lines, 600 lines, 1200 lines, 1800 lines, 2400 lines optional
Detector	1) Deep cooling area array CCD: 2000X256 pixels 2) Deep cooling high sensitivity EMCCD: 1600X200 pixels 3) Deep cooling area array InGaAs CCD: 512X1 pixels Up to 2 detectors can be integrated, choose one from detector 1# or detector 2#;
objective lens	Standard configuration: 4X, 10X, 20X, 50X; Optional configuration: 100X
Microscopic illumination	High brightness and long life white LED
Lighting method	epi-illumination
Microscope camera system	5 million pixel industrial camera
Focus method	conjugate focus
Laser spot diameter	>1 μ m
Laser stability	$\sigma/\mu < \pm 0.2\%$
Communication mode	USB3.0

X, Y axis two-dimensional platform	
Movement method	Fully electric, manual optional
Imaging range	50 X 50 mm, 100 X 100 mm optional
mobile resolution	0.1 μm
positioning accuracy	1 μm
Scan interval	Software settings, minimum 1 μm
Scan speed	20 mm/s
Nanodisplacement stage (optional)	Minimum displacement resolution 2nm, displacement accuracy 10nm
Z axis (auto focus)	
Focus accuracy	$\leq \pm 0.2 \mu\text{m}$
Maximum stroke	20 mm
Focus speed	no more than 10 s
Nanodisplacement stage (optional)	Minimum displacement resolution 2nm, displacement accuracy 10nm
Physical parameters	

size /mm	ATR8800-FL350: 905(L) \times 58.3(W) \times 643(H) ATR8800-FL510: 1009(L) \times 58.3(W) \times 643(H) ATR8800-FL810: 1520(L) \times 68.3(W) \times 643(H)
weight	ATR8800-FL350: 59 Kg ATR8800-FL510: 63 Kg ATR8800-FL810: 78 Kg
Working environment parameters	
Voltage	100~240 VAC
Peak power	< 200 W
Other motivations	No need
emission	none
Platform requirements	Air-floating vibration isolation optical platform
Working temperature and humidity	Constant temperature (25 \pm 2 $^{\circ}$ C), constant humidity (50 \pm 10%)
cleanliness	Level 10,000 and above



Figure 9 ATR8800 type microscopic Raman functional structure indication diagram

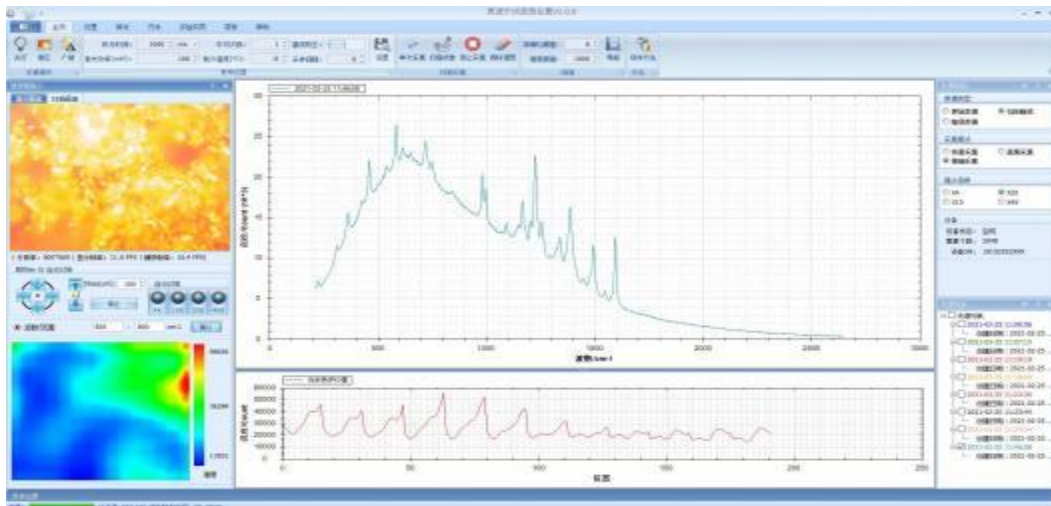


Figure 10 Software interface of ATR8800

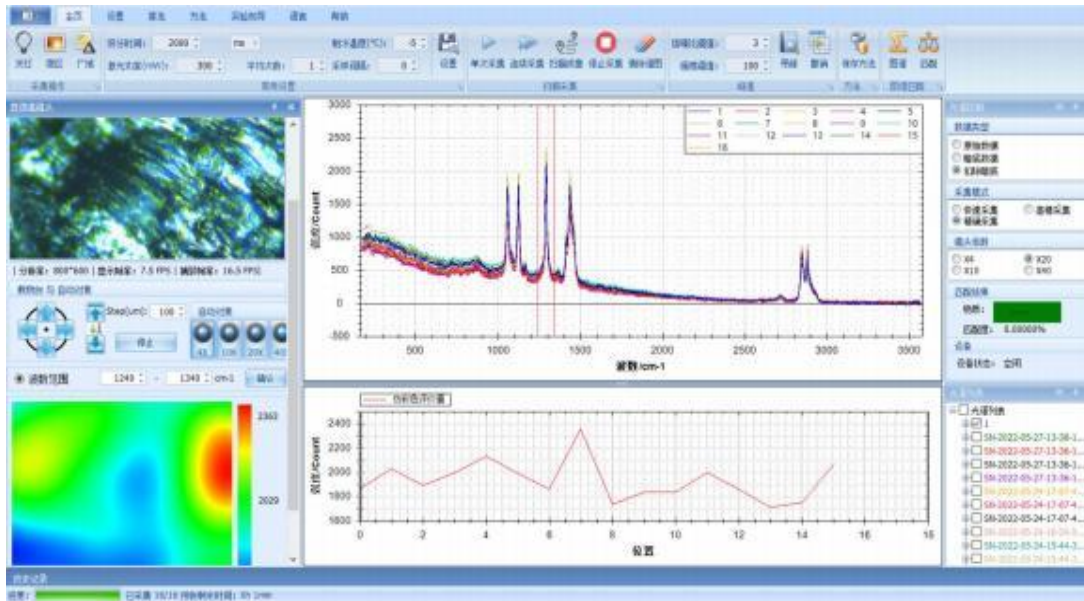


Figure 11 Software interface of ATR8800

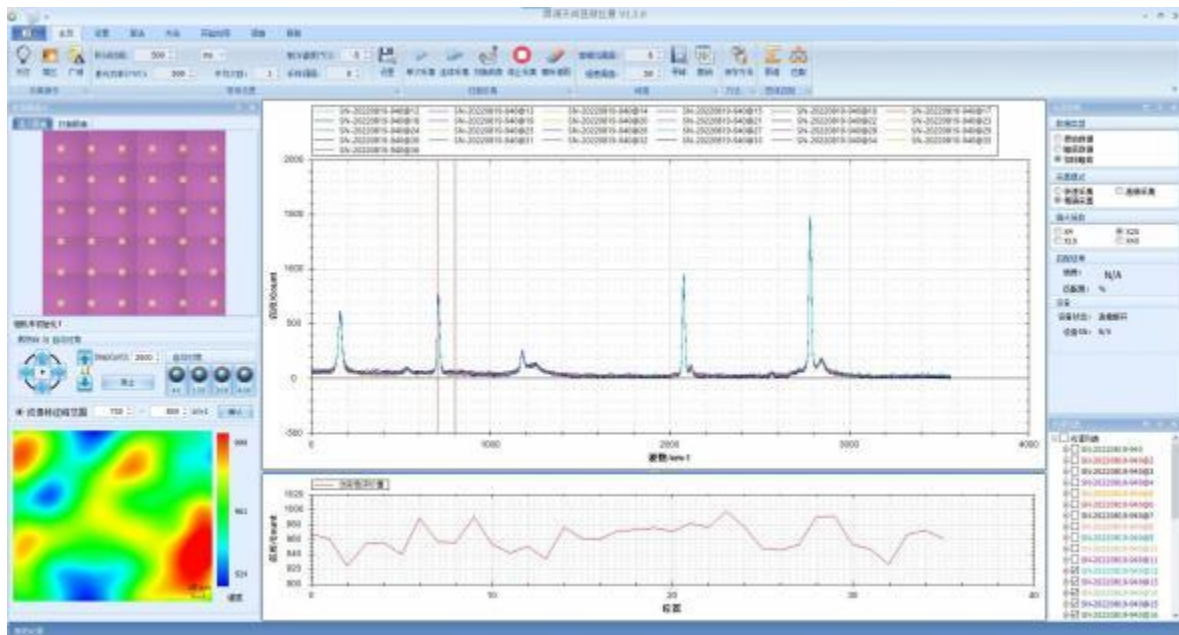


Figure 12 Software interface of ATR8800

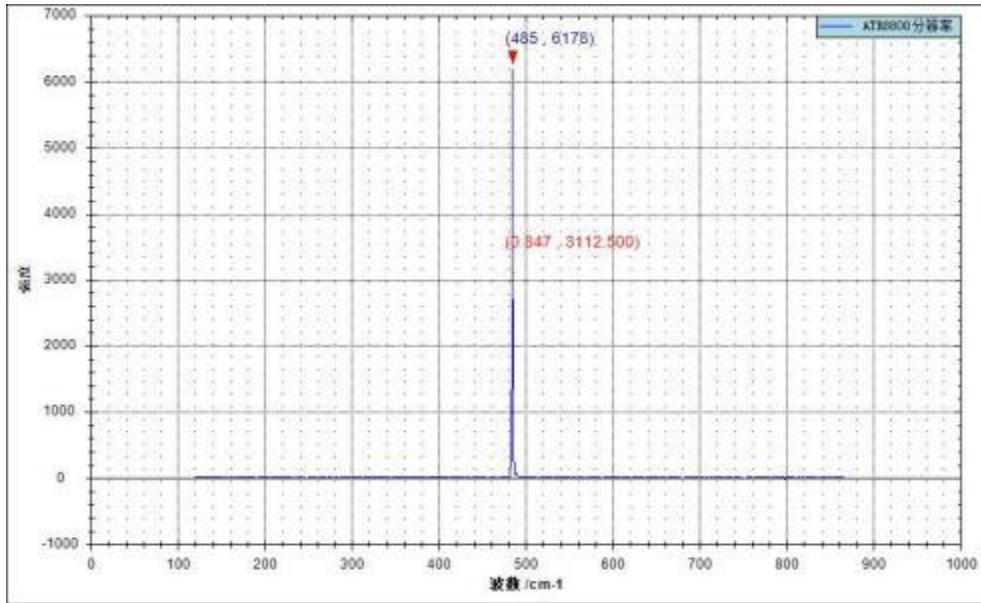


Figure 13 Test results indicate: the instrument resolution reaches 0.847 cm⁻¹, test specification: tested according to the national standard "General Specifications for Raman Spectrometers" method, test equipment: ATR8800-FL510, test light source: mercury argon lamp, collection spectrum line: 546.08 nm

▶ ATR8800的技术特色和竞争优势



- 

01
超快速
自动对焦
- 

02
7个激发波长可选
(从紫外到红外)
- 

03
全自由空间光路,
灵敏度更高
- 

04
自动谱图拼接
(实现高分辨率, 大范围
谱图同时采集)
- 

05
波数实时校准
技术
- 

06
密闭舱门, 做实验
时无需关灯

其他优势

- 1**
- 2**
- 3**
- 4**

1 国产化, 完全自主知识产权

2 交货期短, <3个月

3 **售后服务速度快**
全国各地均有办事处, (24小时内电话响应, 48小时内现场支持)

4 **多种配置可选**
不同腔长, 多种光源, 多种探测器